ELEMENTA
Science of the Anthropocene

Geilfus, N.-X., et al. 2021. Landfast sea ice in the Bothnian Bay (Baltic Sea) as a temporary storage compartment for greenhouse gases. *Elem Sci Anth*, 9: 1. DOI: https://doi.org/10.1525/elementa.2021.00028

RESEARCH ARTICLE

Landfast sea ice in the Bothnian Bay (Baltic Sea) as a temporary storage compartment for greenhouse gases

N.-X. Geilfus[1,*], K. M. Munson[1,2], E. Eronen-Rasimus[3,4], H. Kaartokallio[4], M. Lemes[1], F. Wang[1], S. Rysgaard[1,5], and B. Delille[6]

Although studies of biogeochemical processes in polar sea ice have been increasing, similar research on relatively warm low-salinity sea ice remains sparse. In this study, we investigated biogeochemical properties of the landfast sea ice cover in the brackish Bothnian Bay (Northern Baltic Sea) and the possible role of this sea ice in mediating the exchange of greenhouse gases, including carbon dioxide (CO_2), methane (CH_4), and nitrous oxide (N_2O) across the water column–sea ice–atmosphere interface. Observations of total alkalinity and dissolved inorganic carbon in both landfast sea ice and the water column suggest that the carbonate system is mainly driven by salinity. While high CH_4 and N_2O concentrations were observed in both the water column (up to 14.3 and 17.5 nmol L^{-1}, respectively) and the sea ice (up to 143.6 and 22.4 nmol L^{-1}, respectively), these gases appear to be enriched in sea ice compared to the water column. This enrichment may be attributable to the sea ice formation process, which concentrates impurities within brine. As sea ice temperature and brine volume decrease, gas solubility decreases as well, promoting the formation of bubbles. Gas bubbles originating from underlying sediments may also be incorporated within the ice cover and contribute to the enrichment in sea ice. The fate of these greenhouse gases within the ice merits further research, as storage in this low-salinity seasonal sea ice is temporary.

Keywords: Bothnian Bay, Baltic Sea, Sea ice, CO_2, CH_4, Greenhouse gases

1. Introduction

The Baltic Sea is a brackish subpolar semi-enclosed sea, only connected to the world ocean through the shallow Danish straits, with surface salinity ranging from <1 to 9 (Granskog et al., 2006a). Each winter, sea ice forms and lasts from 5 to 7 months, with a maximum sea ice extent usually observed from mid-February to mid-March. The sea ice cover has large interannual variability in both dates of freezing and break up and its extent and thickness (Granskog et al., 2006a). During mild winters, sea ice only forms in coastal areas and the northernmost basin of the Baltic Sea, the Bothnian Bay (BB), whereas during severe winters, most of the Baltic Sea is ice-covered (Vihma and Haapala, 2015). Due to the brackish nature of its parent seawater, sea ice from the Baltic Sea is characterized by lower bulk ice salinity (usually <2; Granskog et al., 2003) and smaller brine channels (reflecting the brine volume), compared to its polar counterparts. However, while sea ice from the Baltic Sea may be structurally similar to sea ice formed in polar waters, its low salinity (and brine volume content) strongly affects the physical and chemical properties of the ice, with further consequences for biology, remote sensing, and transfer of solutes (e.g., salts, nutrients, gases) across the sea ice–seawater interface. The contribution of meteoric ice (i.e., precipitation transformed into ice) to the total thickness of landfast sea ice in the Baltic can be substantial (Kawamura et al., 2001; Granskog et al., 2006a), as meteoric ice formation is a recurring process in the Baltic Sea. The relatively thin sea ice cover in the Baltic Sea can easily be depressed below seawater level by a small amount of snow deposited onto the ice, resulting in surface sea ice flooding, potentially promoting snow-ice formation. In addition, the mild conditions are favorable for superimposed ice formation by successive melting and refreezing cycles of snow (Granskog et al., 2006a). Depending on the season and year, the meteoric ice fraction has been estimated to contribute up to 35% of the total ice thickness (Granskog et al., 2004).

[1] Centre for Earth Observation Science, Department of Environment and Geography, University of Manitoba, Winnipeg, Manitoba, Canada

[2] Marine and Coastal Research Laboratory, Pacific Northwest National Laboratory, Sequim, WA, USA

[3] Department of Microbiology, University of Helsinki, Helsinki, Finland

[4] Finnish Environment Institute, SYKE, Helsinki, Finland

[5] Arctic Research Center, Aarhus University, Aarhus, Denmark

[6] Chemical Oceanography Unit, Université de Liège, Liège, Belgium

* Corresponding author:
Email: nicolas-xavier.geilfus@umanitoba.ca

As sea ice forms, brine channels and pockets concentrate impurities such as salts, gases, and inorganic and organic components (Eicken, 2003). Once concentrated within sea ice, gas dynamics and fluxes are largely controlled by sea ice temperature and salinity through brine saturation state and sea ice permeability. The resulting chemical activity of these impurities within sea ice influences the exchange of greenhouse gases (GHGs), including carbon dioxide (CO_2), methane (CH_4), and N_2O (notable GHGs), across the ocean–sea ice–atmosphere interface (Lannuzel et al., 2020). During winter, sea ice acts as a source of CO_2 with high brine partial pressure of CO_2 due to increased brine concentrations and associated ikaite precipitation (Rysgaard et al., 2011; Geilfus et al., 2013; Fransson et al., 2015; Geilfus et al., 2016), whereas in spring and summer, sea ice shifts to become a sink for atmospheric CO_2 due to brine freshening, ikaite dissolution, and the biological carbon pump (Rysgaard et al., 2011; Geilfus et al., 2012; Van der Linden et al., 2020).

Relative to CO_2, the impact of sea ice on CH_4 exchange across the ocean–sea ice–atmosphere interface is less well understood. Sea ice has been suggested to play a key role on the regulation of CH_4 concentrations in the Arctic. In winter, CH_4 has been reported to accumulate either within the sea ice matrix (Shakhova et al., 2010; Crabeck et al., 2014) or at its interface with the water column (Kvenvolden et al., 1993; Kitidis et al., 2010). As sea ice temperature increases, CH_4 could be released, either directly to the atmosphere (Shakhova et al., 2010) or to the underlying seawater, along with the brine drainage (Damm et al., 2015). Sea ice melt decreases the saturation state of surface water, resulting in a drawdown of atmospheric CH_4 (Heeschen et al., 2005). However, sea ice can also enhance CH_4 oxidation, potentially reducing CH_4 effluxes to the atmosphere (Tison et al., 2017), particularly above continental shelves where sediment represents the main source of CH_4 to the ocean (Arctic Monitoring and Assessment Programme, 2015), and significant ebulliative fluxes are reported (Shakhova et al., 2010). The major CH_4 sources in marine systems are microbial methanogenesis in anaerobic sediments and abiotic geochemical processes (Reeburgh, 2007). Usually a large fraction (up to 90%) of released CH_4 is oxidized in microbially mediated processes before it reaches the upper water layers (Reeburg, 2007; Knittel and Boetius, 2009). In addition to anaerobic methanogenesis, CH_4 can also be produced in aerobic conditions via methylotrophic methanogenesis when bacteria use methylphosphonate as their phosphate source, releasing CH_4 (Karl et al., 2008; Carini et al., 2014). Highest CH_4 emissions occur in coastal areas of high organic matter input from rivers (Humborg et al., 2019). In the Baltic Sea, lateral transport of CH_4 via riverine flow can also significantly contribute to high coastal concentrations and CH_4 supersaturation (Myllykangas et al., 2021). Eutrophication and global warming are suggested to increase CH_4 release to the atmosphere (Borges et al., 2016; Humborg et al., 2019).

N_2O production, mainly occurring in sediments, is regulated by the presence of oxygen and nitrogen availability. Microbial N_2O production is complex and takes place in multiple oxidative and reductive processes of the nitrogen cycle (Anderson and Levine, 1986; Bakker et al., 2014). Estuaries and coastal areas are known to be areas for high N_2O production due to high riverine loads of nitrogen (Bakker et al., 2014). Fewer studies have investigated N_2O cycling in the Arctic, and the N_2O cycle within sea ice is relatively unknown. Sea ice growth and melt (Kitidis et al., 2010; Randall et al., 2012) as well as denitrification and diazotrophy (Verdugo et al., 2016) have been suggested to affect the N_2O cycle and the exchanges of N_2O with both the atmosphere and the water column (Kaartokallio, 2001). The sea ice bacterial community harbors potentially denitrifying organisms (Deming and Collins, 2017); however, identification of active denitrifying microbes and their prevalence remain areas of ongoing research.

GHGs are produced and/or consumed by diverse assemblages of auto- and heterotrophic organisms living in or under the ice during the annual cycle of sea ice growth and melt (Arrigo, 2017; Bluhm et al., 2017; Caron et al., 2017; Deming and Collins, 2017; Lannuzel et al., 2020). Bacteria are the main group of organisms responsible for decomposing organic matter and remineralizing the nutrients, and their growth is regulated by multiple simultaneously acting environmental factors, such as salinity, temperature, and nutrients (Pomeroy and Wiebe, 2001; Kuosa and Kaartokallio, 2006), as well as food web interactions, such as protistan grazing (Kaartokallio, 2004; Riedel et al., 2007). Baltic and Arctic sea ice bacterial communities harbor potential methane-oxidizing bacteria, such as *Methyloacidophilaceae* (E Eronen-Rasimus, personal communication, September 2021; Op den Camp et al., 2009) and the genus *Methylomicrobium* (Bowman et al., 2012; Puri et al., 2015); however, their abundance is low, and their methane oxidation activity within the ice has not been verified.

While sea ice plays an active role in GHG exchange (Rysgaard et al., 2011; Geilfus et al., 2012), more extensive study is needed to determine the magnitudes and controls of that exchange (Parmentier et al., 2017; Lannuzel et al., 2020). Biogeochemical processes at low salinity and warm temperature potentially differ from those in polar seas but are absent from published data sets. To our knowledge, we present the first observations of GHG dynamics within sea ice in the BB and how sea ice could affect GHG exchanges across the ocean–sea ice–atmosphere interface. Due to the low salinity in the Baltic Sea, its sea ice could potentially be used as a model to investigate future changes in Arctic sea ice due to warming associated with climate change, especially on shallow shelves where high river inputs can significantly reduce sea surface salinity (Granskog et al., 2006a). Therefore, we investigated how landfast sea ice in the BB controls the exchange of GHGs across the ocean–sea ice–atmosphere and relate our observations to the current understanding of microbial production within the ice cover.

2. Methods

2.1. Study area

Sea ice and seawater samples were collected in the northernmost basin of the Baltic Sea, the BB. This shallow basin,

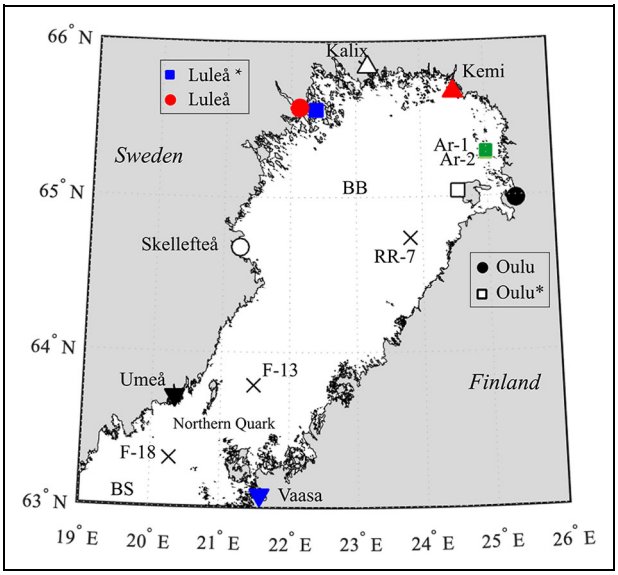

Figure 1. Sampling locations in the Bothnian Bay and Bothnian Sea, Northern Baltic Sea. Sampling sites for sea ice (colored symbols) and seawater (black crosses) in the Bothnian Bay (BB) and Bothnian Sea (BS). DOI: https://doi.org/10.1525/elementa.2021.00028.f1

with an average depth of 43 m, is separated from the deeper southern basin of the Gulf of Bothnia, the Bothnian Sea (BS), by the Northern Quark, a shallow sill of only 20 m depth (**Figure 1**). The brackish nature of the seawater in both basins is due to the high riverine discharge from large catchments and limited supply of saline water from lateral intrusions of surface water from the central Baltic Sea. Mean seawater surface salinity is 3.5 in the BB and slightly higher at 6.5 in the BS due to larger inflow of saline waters from the Baltic Proper (Löffler et al., 2012).

Samples were collected from 9 landfast sea ice stations from the Swedish and Finnish coasts (**Figure 1**; **Table 1**) from 18 to 25 February 2018. Sampling locations were chosen close to riverine inputs and major cities as part of a research program dedicated to microplastic incorporation within sea ice (Geilfus et al., 2019). In Luleå (Sweden) and Oulu (Finland), sea ice was also collected away from the river geographically (noted as Luleå* and Oulu*). Additional landfast sea ice (stations Ar-1 and Ar-2) and seawater samples (stations RR-7, F-13, and F-18) were collected onboard the R/V *Aranda*, from 3 to 5 February 2020, as part of the annual winter monitoring cruise COMBINE 1. All sea ice samples were collected in shallow areas, as samples from 2018 were collected by walking from the seashore while the water depths at stations Ar-1 and Ar-2 were 21 and 22 m, respectively.

2.2. Sampling procedure

Sea ice cores were collected using a MARK II coring system (internal diameter = 9 cm, Kovacs Enterprises®, Roseburg, OR, USA). Directly after extraction of the core, the temperature profile was measured in situ using a calibrated temperature probe (Testo 720®, ±0.1°C precision) inserted into predrilled holes (5-cm intervals), perpendicular to core sides. Cores were then cut into 5–10 cm sections, stored in sealed plastic containers, and vacuum-sealed in a gas-tight plastic bag (nylon/poly, Cabela's, Sidney, NE, USA; Hu et al., 2018) directly in the field. Back in the laboratory, samples were melted in the dark at 4°C to minimize the possible dissolution of ikaite crystals. Once melted, aliquots of meltwater were transferred into 12-ml gas-tight vials (Exetainers, Labco, High Wycombe, United Kingdom) for total alkalinity (TA) and dissolved inorganic carbon (DIC) measurements, while CH_4 and N_2O samples were collected into 60-ml serum bottles. Samples were preserved by adding 20 and 60 µL, respectively, of a saturated mercuric chloride ($HgCl_2$, Thermo Fisher [Kandel] GmbH, Germany) solution. Water aliquots (2 mL) were also collected in glass vials without head space for stable isotope composition of oxygen in water, $\delta^{18}O$-H_2O, herein referred to as $\delta^{18}O$. Samples were then stored in the dark at room temperature until analysis.

Seawater samples were collected onboard R/V *Aranda* using a rosette sampling system equipped with 24 12-L Niskin-type bottles (Sea-Bird PVC sample bottle) and probes for conductivity, temperature, and depth (CTD Sea-Bird SBE-911+, calibrated by the manufacturer). Conductivity drift was checked and corrected, based on discrete water samples taken throughout the water column and analyzed onboard using a Guildline Autosal 8400 salinometer calibrated with standard seawater from the International Association for Physical Sciences of the Ocean. Samples for TA, DIC, CH_4, N_2O, and $\delta^{18}O$ were collected, following the same procedure as for melted sea ice, immediately after the rosette was secured onboard.

2.3. Sample analysis

Bulk ice salinity was calculated based on conductivity (Grasshoff et al., 1983) measured using a meter (Orion 3-star, Thermo Scientific, Waltham, MA, USA) coupled with a conductivity cell (Orion 013610MD, Thermo Scientific). Brine volume was estimated from measurements of bulk ice salinity, temperature, and density according to Cox and Weeks (1983) for temperatures below –2°C and according to Leppäranta and Manninen (1988) for ice temperatures within the range of –2°C to 0°C.

TA was determined by Gran titration (Gran, 1952) using a TIM 840 titration system (Radiometer Analytical, ATS Scientific, Burlington, Ontario, Canada), consisting of a Ross sure-flow combination pH glass electrode (Orion 8172BNWP, Thermo Scientific) and a temperature probe (Radiometer Analytical, Lyon, France). A 12-mL sample was titrated with a standard 0.05 M HCl solution (Alfa Aesar, Ward Hill, MA, USA). DIC was measured on a DIC analyzer (Apollo SciTech, Newark, DE, USA) by acidification of a 0.75-mL subsample with 1 mL 10% H_3PO_4 (Sigma-Aldrich, Saint-Louis, MO, USA), and quantification of the released CO_2 with a nondispersive infrared CO_2 analyzer (LI-7000, LI-COR, Lincoln, NE). Results were then converted from µmol L^{-1} to µmol kg^{-1} based on sample density, which was estimated from salinity and temperature at the time of the analysis. Accuracies of ±3 and ±2 µmol kg^{-1} were determined for TA and DIC, respectively, from routine analysis of certified reference materials (AG Dickson, Scripps Institution of

Table 1. Sampling date, location, and associated sea ice and snow thickness as well as freeboard. DOI: https://doi.org/10.1525/elementa.2021.00028.t1

Date (dd/mm/yyyy)	Stations	Latitude (N)	Longitude (W)	Sea Ice Depth (cm)	Snow Depth (cm)	Freeboard (cm)
18/02/2018	Luleå*	65°33′54″	22°23′24″	38	45	9
18/02/2018	Skelleftea	64°40′30″	21°14′35″	35	16	2
19/02/2018	Kalix	65°51′02″	23°08′10″	42	48	na
19/02/2018	Luleå	65°34′33″	22°07′55″	35	45	9
20/02/2018	Kemi	65°40′30″	24°31′02″	34	28	2
21/02/2018	Oulu*	65°02′10″	24°33′15″	30	4	−2
23/02/2018	Oulu	64°58′59″	25°25′44″	44	9	1
24/02/2018	Vaasa	63°04′41″	21°34′58″	34	10	2
25/02/2018	Umeå	63°42′42″	20°19′47″	46	14	−2
03/02/2020	Ar-1	65°16′34″	25°0′11″	45	2	na[a]
04/02/2020	Ar-2	65°17′19″	24°59′46″	42	2	na
05/02/2020	RR-7	64°44′1″	23°48′46″	na	na	na
05/02/2020	F-13	63°47′0″	21°28′46″	na	na	na
05/02/2020	F-18	63°18′52″	20°16′22″	na	na	na

[a]Parameters not measured or not applicable.

Oceanography, San Diego, CA, USA). CH_4 and N_2O concentrations were measured via the headspace equilibrium technique (25 ml N_2 headspace in 60-ml serum bottles) and measured with a gas chromatograph (SRI 8610C) with flame ionization detection, and electron capture detection calibrated with CH_4: CO_2: N_2O: N_2 mixtures (Air Liquide, Paris, France) of 1, 10, and 30 ppm CH_4 and 0.2, 2.0, and 6.0 ppm N_2O. The measurement precision was 3.9% for CH_4 and 3.1% for N_2O. Values for $\delta^{18}O$ were measured on an isotope analyzer (L2130-*i*, Picarro, Santa Clara, CA, USA) with a precision of 0.025‰, calculated as the standard deviation (*SD*) from 10 repeated measurements of standard materials.

3. Results

3.1. Sea ice

Sea ice thickness ranged from 30 to 46 cm (**Figure 2**; **Table 1**) and exhibited a typical temperature gradient, with colder temperatures observed at the sea ice interface with the atmosphere (minimum of −7.1°C at Ar-2). Bulk ice salinity was typical for the Baltic Sea (Granskog et al., 2006a), with values lower than 1. Due to the low salinity, the brine volume content of the ice was below the permeability threshold (5%; Golden et al., 2007; **Figure 2d**). Sea ice $\delta^{18}O$ ranged from −18.7‰ to −7.8‰. Lowest values were observed in the upper section of the ice cover. The $\delta^{18}O$ increased downward throughout the ice cover and remained relatively constant toward the bottom of the cores (mean = −10.1‰, SD = 1.1, n = 22), except at Oulu* where the $\delta^{18}O$ profile remained relatively constant throughout the entire ice thickness with averaged $\delta^{18}O$ less depleted than at other stations (Oulu*: −8.3‰; **Figure 2c**).

Concentrations of TA and DIC ranged from 18 to 282 μmol kg^{-1} and from 12 to 267 μmol kg^{-1}, respectively (**Figure 3**). These concentrations fall at the low end of previously reported values in Arctic sea ice (Rysgaard et al., 2007; Geilfus et al., 2015; Fransson et al., 2017) but are comparable to values reported from multiyear sea ice (Rysgaard et al., 2009; Geilfus et al., 2021) and expected from the low bulk ice salinity. Oulu* stands out of the general pattern with higher concentrations of both TA and DIC compared to the other stations. No general pattern could be observed in the TA and DIC profiles. The sea ice surface has either maximum concentrations of TA and DIC (Skellefteå, Kemi, and Oulu*) or minimum concentrations (Luleå, Umeå, Oulu, Ar-1, and Ar-2). Finally, concentrations at the Kalix and Vaasa sites appear homogeneous throughout the ice thickness.

Concentrations of CH_4 ranged from 2.6 to 143.6 nmol L^{-1} (**Figure 3**), up to 10 times the sea ice CH_4 concentration reported in a Greenlandic fjord (Crabeck et al., 2014) or in landfast sea ice in Barrow, Alaska (Zhou et al., 2014). Maximum concentrations were observed at the sea ice interface with the atmosphere at Skellefteå, Umeå, Oulu, Vaasa, and Ar-1, which contrasts with Luleå, Kalix, Kemi, and Oulu*, where CH_4 profiles remained constant throughout the ice thickness. Bottom CH_4 concentrations for all stations were in the same range (mean = 7.9 nmol L^{-1}, SD = 3.6, n = 22), except at Vaasa where the highest concentration was observed (143.6 nmol L^{-1}). N_2O concentrations ranged from 3.2 to 22.4 nmol L^{-1}, with the highest concentrations (>10 nmol L^{-1}) observed at Vaasa. Local maxima were observed at the upper layer of the ice surface, except at Luleå* and Oulu*.

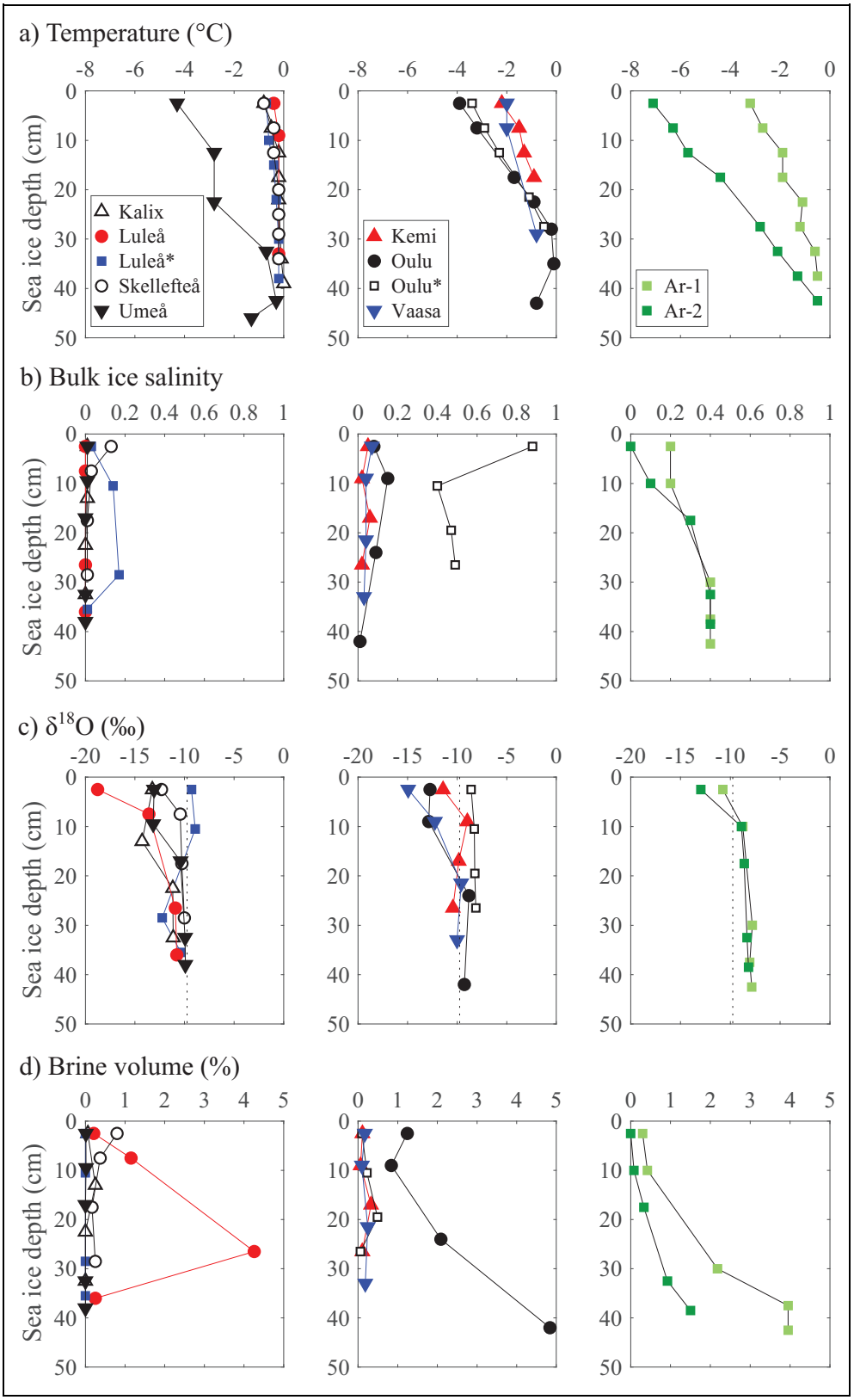

Figure 2. Sea ice profiles of temperature, bulk ice salinity, $\delta^{18}O$, and brine volume. Data symbols are shape- and color-coded by station (locations in **Figure 1**) for (a) temperature (°C), (b) bulk ice salinity, (c) $\delta^{18}O$ (‰), and (d) brine volume (%). The dotted line on each graph in Panel c represents the averaged $\delta^{18}O$ of surface seawater. DOI: https://doi.org/10.1525/elementa.2021.00028.f2

3.2. Water column

The water column of the BB was sampled at stations RR-7 and F-13, while the BS was sampled at station F-18 (**Figure 1**). In the BB, the water column was quite homogeneous, without a thermocline or halocline observed (**Figure 4**). Seawater temperature was <1°C (mean = 0.64, *SD* = 0.29,

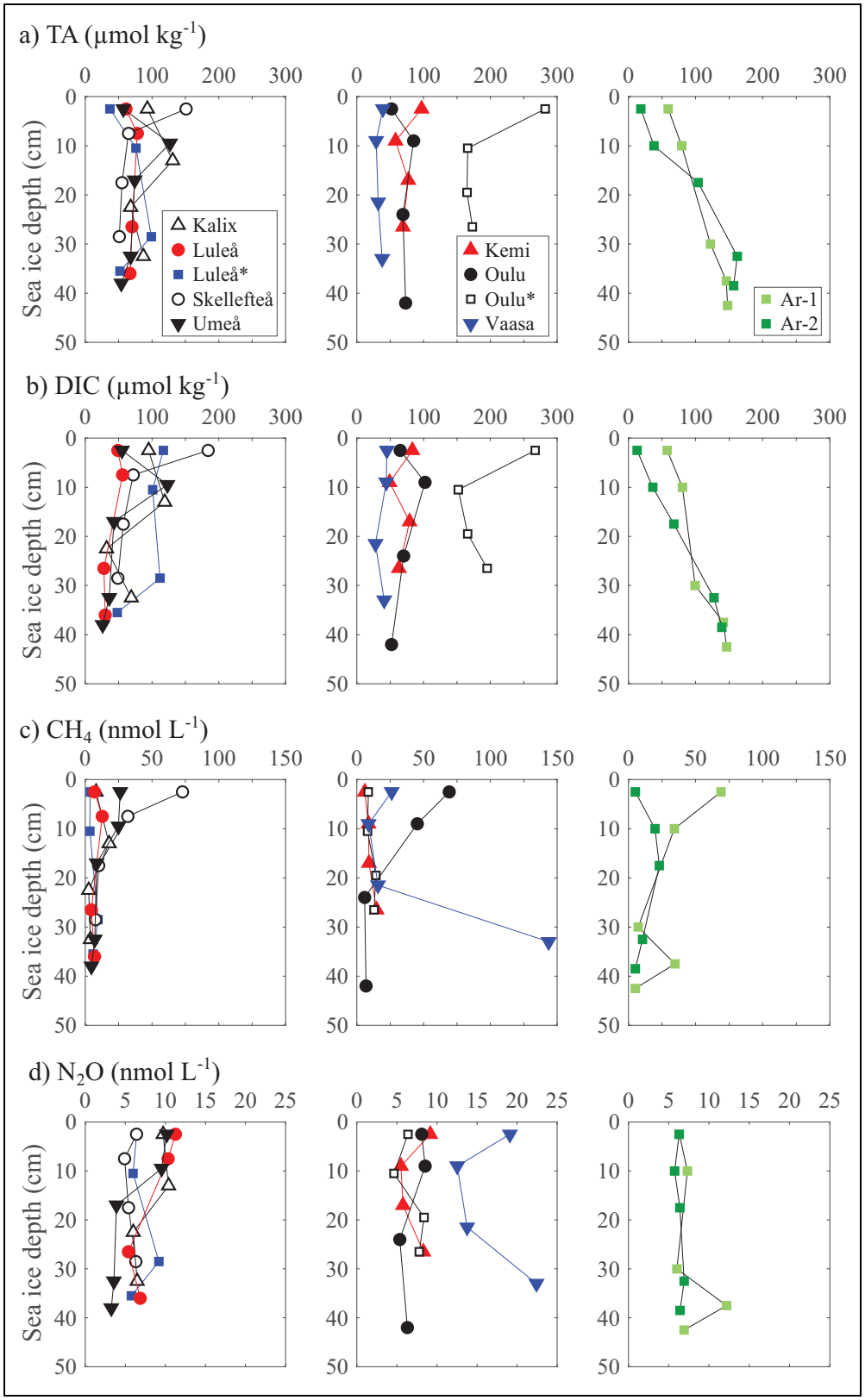

Figure 3. Sea ice profiles of total alkalinity, dissolved inorganic carbon, CH_4, and N_2O concentrations. Data symbols are shape- and color-coded by station (locations in **Figure 1**) for (a) total alkalinity (TA, µmol kg^{-1}), (b) dissolved inorganic carbon (DIC, µmol kg^{-1}), (c) CH_4 (nmol L^{-1}), and (d) N_2O (nmol L^{-1}) concentrations. DOI: https://doi.org/10.1525/elementa.2021.00028.f3

$n = 16$), and its salinity averaged 3.21 ($SD = 0.09$, $n = 16$). However, at F-13, seawater temperature and salinity increased slightly with depth from 0.8°C and 3.21°C, respectively, at the surface to 0.96°C and 3.42°C, respectively, at the bottom. At F-18, both a thermo- and halocline were observed at 40–50 m depth (**Figure 4**). The

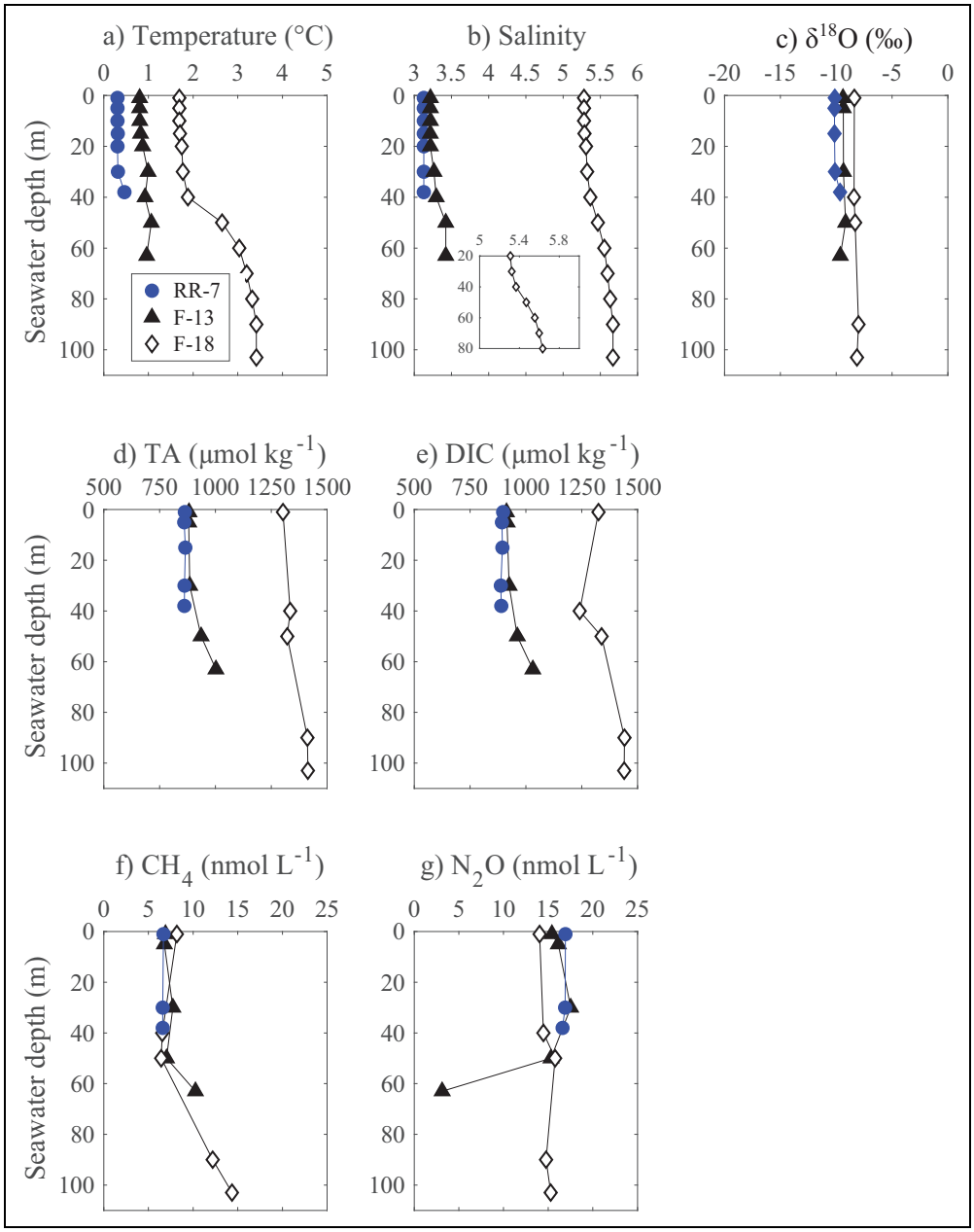

Figure 4. Seawater profiles of the parameters measured. Data symbols are shape- and color-coded for the 3 stations sampled (inset legend in Panel a; locations marked by black crosses in **Figure 1**) for (a) temperature (°C), (b) salinity, (c) $\delta^{18}O$ (‰), (d) total alkalinity (TA, µmol kg^{-1}), (e) dissolved inorganic carbon (DIC, µmol kg^{-1}), (f) CH_4 (nmol L^{-1}), and (g) N_2O (nmol L^{-1}) concentrations. The inset in Panel b is to help visualize the halocline at 40–50 m. DOI: https://doi.org/10.1525/elementa.2021.00028.f4

upper layer had an average temperature and salinity of 1.73°C ($SD = 0.07$, $n = 7$) and 5.29°C ($SD = 0.02$, $n = 7$), respectively, while the bottom layer averaged 3.27°C ($SD = 0.16$, $n = 6$) and 5.56°C ($SD = 0.11$, $n = 6$), respectively. Values for $\delta^{18}O$ were stable throughout the water column at each station, with averaged values increasing from −10.0‰ at RR-7 ($SD = 0.2$, $n = 5$) to −9.4‰ at F-13 ($SD = 0.1$, $n = 5$), and −8.2‰ ($SD = 0.1$, $n = 5$) at F-18.

In the BB, TA and DIC concentrations were similar between stations, with TA ranging from 860 to 1002 µmol kg^{-1}, and DIC ranging from 888 to 1031 µmol kg^{-1}. In the BS (F-18), TA and DIC increased with concentrations ranging from 1302 to 1414 µmol kg^{-1} and from 1241 to 1441 µmol kg^{-1}, respectively. Profiles of CH_4 and N_2O concentrations were quite similar between stations. CH_4 concentrations in the upper 50 m were on average at 6.8 nmol L^{-1} ($SD = 0.6$, $n = 6$). At both F-13 and F-18, an increase in CH_4 concentration (up to 14.3 nmol L^{-1}) with depth was observed. Based on seawater temperature, salinity, CH_4 concentration, and using constants from Wiesenburg and Guinasso (1979), we estimated that surface waters in both the BB and BS were supersaturated with CH_4 (up to 176%) compared to the atmosphere. N_2O concentrations were stable between stations with the concentration averaging 14.8 nmol L^{-1} ($SD = 3.7$, $n = 13$), with a low concentration of 3.1 nmol L^{-1} observed at the bottom of F-13. Based on

constants from Weiss and Price (1980), we determined that the surface water was undersaturated in N_2O compared to the atmosphere.

4. Discussion

4.2. Sea ice properties

The sea ice conditions encountered during this survey were typical for the Baltic Sea (Granskog et al., 2006a), where the low bulk ice salinity is mainly due to the brackish nature of the parent seawater (**Figure 4**). However, the presence of snow and/or superimposed ice on the sea ice cover also potentially affects the bulk ice salinity. The strongly depleted $\delta^{18}O$ values observed in the upper layer of the ice cover (**Figure 2**) could suggest the presence of meteoric ice in our samples. Meteoric water distributions from riverine sources were not differentiated due to the lack of endmember or ice texture analysis. The upper 10–30 cm of the ice cover exhibited more depleted $\delta^{18}O$ values compared to the averaged $\delta^{18}O$ of surface seawater in the BB (–9.75‰; dotted line, **Figure 2c**). This difference could indicate the presence of meteoric ice formation, either due to snow ice formation or surface flooding by local river runoff, except at Oulu* where the $\delta^{18}O$ profile within sea ice was more homogeneous and less depleted (mean = –8.3‰) compared to the average surface seawater.

4.2. Biogeochemical processes within sea ice

The low TA and DIC concentrations within sea ice are expected due to low bulk ice salinity, as TA and DIC in both sea ice and seawater exhibited a strong correlation with salinity (black dotted line, **Figure 5**). Most of the TA:DIC data from both seawater and sea ice align on the slope of 1 (dashed black line, **Figure 5c** and **f**), except the upper sea ice layer in Luleå (blue square, **Figure 5f**). As no ikaite precipitates were observed during the sea ice melt, this alignment confirms a lack of precipitation of calcium carbonate within sea ice, which contrasts with polar sea ice where ikaite is commonly reported (Dieckmann et al., 2008; Geilfus et al., 2013; Rysgaard et al., 2013). Taking into account the low bulk sea ice salinity (<1) and related brine volume fraction below the sea ice permeability threshold (5%; Golden et al., 2007), sea ice in the BB appears to mimic the "closed system" of sea ice formation, unfavorable for ikaite precipitation (Papadimitriou et al., 2013). In such a system, rejection of excess CO_2 from sea ice does not occur and thus the low pCO_2 needed for ikaite to precipitate is not maintained (Papadimitriou et al., 2013). In addition, precipitation of calcium carbonate within the water column has been suggested to be negligible in the BB and BS due to undersaturation of both calcite and aragonite minerals in winter (Tyrrell et al., 2008).

Within sea ice, both TA and DIC exhibited large variability compared to their relationship with salinity (**Figure 5d** and **e**). Based on averaged surface seawater TA (871 μmol kg^{-1}, $SD = 13$, $n = 4$) and DIC (905 μmol kg^{-1}, $SD = 10$, $n = 4$) in the BB, we calculated the expected surface seawater TA and DIC at salinities observed within sea ice (from 0.1 to 0.9) considering that TA and DIC are conservative with salinity (red dashed line, **Figure 5d** and **e**). Most of the sea ice data exhibited higher TA and DIC than expected in seawater at similar salinity values, suggesting an enrichment in the ice cover compared to the underlying seawater. However, the sea ice data covered a large part of the BB, while seawater was only sampled twice in the BB (at RR-7 and F-13). RR-7 was sampled not too far away from Oulu, Oulu*, Ar-1, and Ar-2, and both RR-7 and F-13 exhibited similar properties (**Figure 4**). This sea ice enrichment was also observed for both CH_4 and N_2O (**Figure 6**). CH_4 concentrations within sea ice were an order of magnitude higher than those observed within the water column (**Figure 6a**). To account for CH_4 and N_2O from parent seawater, we normalized the averaged surface seawater concentration of CH_4 (6.8 nmol L^{-1}, $SD = 0.1$, $n = 3$) and N_2O (16.1 nmol L^{-1}, $SD = 1.0$, $n = 3$), observed in the BB to a bulk ice salinity of 0.5 (noted as nCH_{4_sw} and $nN_2O_{\_sw}$). CH_4 concentrations within sea ice were significantly higher than nCH_{4_sw} (1.0 nmol L^{-1}; red line, **Figure 6c**), suggesting a CH_4 enrichment within sea ice compared to the underlying seawater. N_2O concentrations within sea ice are the same order of magnitude as those in the water column (**Figure 6b**). However, $nN_2O_{\_sw}$ (2.5 nmol L^{-1}) is lower than observed sea ice concentrations, also suggesting an enrichment of N_2O within sea ice compared to the underlying seawater (**Figure 6d**).

As sea ice forms, it concentrates impurities, including gases, within the ice structure (Eicken, 2003). Therefore, high GHG concentrations within sea ice could originate from the parent seawater. If the carbonate system follows the dilution curve (**Figure 5**), then high CH_4 and N_2O concentrations are observed in the water column (**Figure 4**). CH_4 supersaturation has been reported across the Baltic Sea (Bange et al., 1994; Schmale et al., 2010), with CH_4 concentrations increasing with seawater depth (**Figure 4**), suggesting a release of CH_4 from the sediment to the water column (Schmale et al., 2010). Another source of GHGs to the marine environment could be the waters discharged from rivers (Frankignoulle et al., 1998; Borges, 2005). In Liminganlahti Bay, south of Oulu, CO_2 and CH_4 supersaturation has been observed in river water during wintertime and has been associated with the lack of photosynthesis and the presence of river ice impeding gas exchange with the atmosphere (Silvennoinen et al., 2008). Apart from the river water layer, lowest CH_4 concentrations were observed during winter, suggesting other controls than solubility (Myllykangas et al., 2021). However, riverine contributions to TA in the Baltic Sea are spatially variable and depend on the bedrock nature of the catchment area (Schneider, 2011). In the Gulf of Bothnia, riverine contributions to TA ranged from 140 to 229 μmol kg^{-1} (Hjalmarsson et al., 2008, and Beldowski et al., 2010, respectively). This small contribution is mainly due to igneous rock in the catchment areas that does not release weathering products contributing to TA (Löffler et al., 2012). From **Figure 5**, the contribution of river water (salinity = 0) in TA and DIC can be estimated at 45 and 41 μmol kg^{-1}, respectively, suggesting a minor

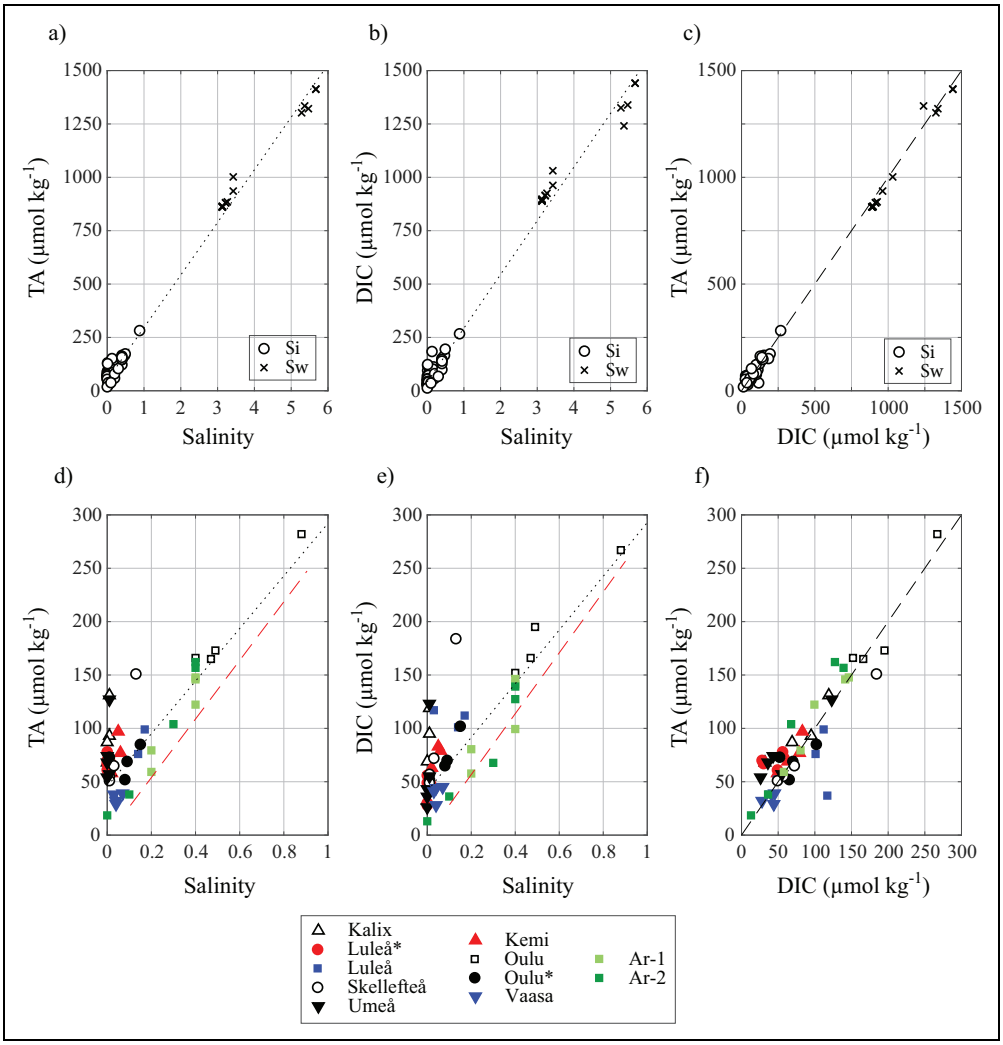

Figure 5. Relationships between total alkalinity, dissolved inorganic carbon, and salinity in sea ice and seawater. Upper panels present, for both sea ice (Si) and seawater (Sw), the relationships between (a) total alkalinity (TA, µmol kg^{-1}) and salinity, (b) dissolved inorganic carbon (DIC, µmol kg^{-1}) and salinity, and (c) TA and DIC. Corresponding lower panels depict the sea ice data using symbols shape- and color-coded by station (inset legend; locations in **Figure 1**). The dotted black line in Panels a, b, d, and e represents the dilution line. The dashed black line in Panels c and f represents the DIC: TA ratio of 1. The red dashed line in Panels d and e represents an estimate of what surface seawater TA and DIC would be at similar salinity observed within sea ice (from 0.1 to 0.9), considering TA and DIC conservative with salinity. DOI: https://doi.org/10.1525/elementa.2021.00028.f5

contribution of riverine water to the carbonate system in the marine environment.

In addition to their enrichment from either riverine or marine waters, GHGs may accumulate in sea ice from bubbles. As sea ice temperature decreases, the brine volume decreases with the potential to affect pressure, bubbles, and the solubility of gases trapped within sea ice (Crabeck et al., 2019). Gas supersaturation leads to bubble nucleation (Zhou et al., 2013). Because gas bubbles move upward due to their buoyancy, while dissolved compounds are subject to gravity drainage (i.e., downward movement), gas bubble formation can drive gas accumulation in sea ice (Zhou et al., 2014). The enrichment of CH_4 in sea ice could be due to CH_4 bubbles released from the sediment that migrate through the water column due to their own buoyancy and accumulate within the ice structure as sea ice grows.

Vertical profiles of CH_4 concentration in sea ice exhibit maximum concentrations in the upper layer (**Figure 3**), except at Vaasa where an increase in CH_4 concentration was observed at the surface but the maximum value was at the sea ice bottom. The increase of gas concentration at the surface is less marked for N_2O and DIC than for CH_4. Excess of CH_4 at the ice surface could be associated with the formation of meteoric ice due to the flooding of CH_4-supersaturated river water onto the ice surface. In addition, an enhanced ebullition flux of CH_4 early in the ice formation could contribute to the higher CH_4 concentrations. In fall, organic matter from the summer phytoplankton bloom and relatively high bottom water temperatures may support significant benthic mineralization (Humborg et al., 2019). Decrease of CH_4 ebullition fluxes from fall to winter has been documented for temperate continental aquatic systems (Wilkinson et al., 2015; Tušer et al., 2017)

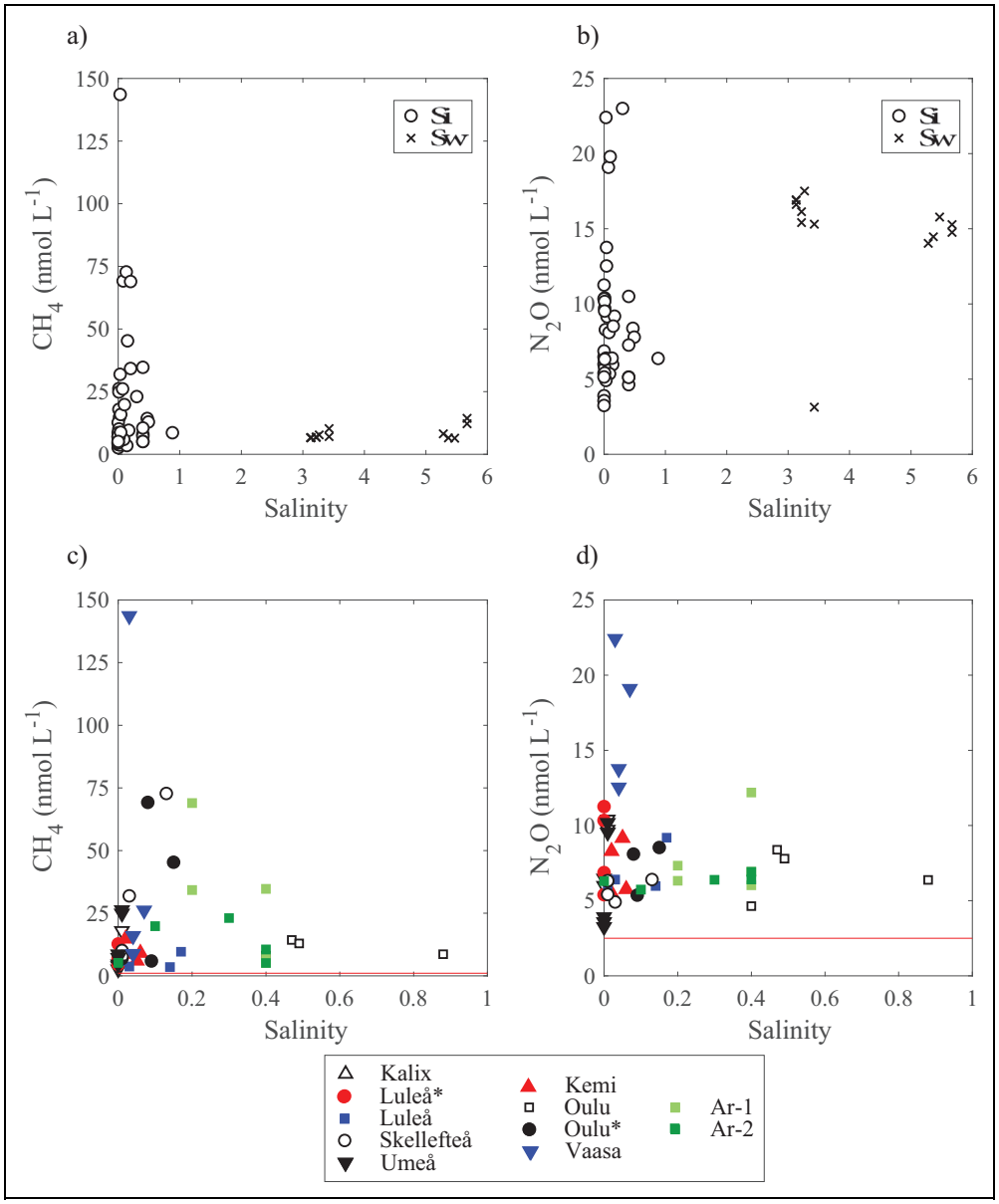

Figure 6. Relationships between salinity and CH_4 and N_2O in sea ice and seawater. Upper panels present, for both sea ice (Si) and seawater (Sw), the relationships between (a) CH_4 (nmol L^{-1}) and salinity, (b) N_2O (nmol L^{-1}) and salinity. Corresponding lower panels depict the sea ice data using symbols shape- and color-coded by station (inset legend; locations in **Figure 1**). The red (dotted) line in Panels c and d represents the CH_4 or N_2O concentrations expected in surface seawater at a salinity of 0.5. DOI: https://doi.org/10.1525/elementa.2021.00028.f6

and could explain the decrease in CH_4 concentrations with sea ice depth, associated with the slower growth rate of the ice as it thickens, increasing the efficiency of impurity rejection (salts, gases) to the water column as sea ice grows (Granskog et al., 2006b).

Once GHGs are trapped within the ice structure, gas bubbles will not escape to the atmosphere as long as the sea ice permeability is low (e.g., brine volume < 5%; Golden et al., 2007), and GHGs could remain within the ice matrix until the onset of sea ice melt. CH_4 temporarily trapped within the ice structure or under-ice water could be subject to microbial oxidation to CO_2 within sea ice and meltwater and buffered by the carbonate system of the ocean. However, the prevalence and activity of the potential CH_4 oxidizers need to be verified in future studies. Nevertheless, our results suggest that sea ice in the BB could act as a sink for CH_4, whereas the increasing temperatures and loss of sea ice cover due to global warming may increase CH_4 fluxes in the Baltic Sea (Humborg et al., 2019).

5. Conclusions

While the role of sea ice in GHG exchanges across the ocean–sea ice–atmosphere interface is poorly constrained, observations over brackish sea ice, as in the BB, are still lacking. Due to ongoing changes in the polar regions, with undefined consequences for sea ice biogeochemical cycles (Lannuzel et al., 2020), investigations of low salinity sea ice in the Baltic Sea may help to constrain future changes in the warming Arctic, especially on shallow shelves where

increased freshwater input can significantly reduce sea surface salinity.

The carbonate system of both sea ice and the water column in this study appeared to be driven mainly by salinity. High CH_4 and N_2O concentrations were observed in both sea ice and the water column, but the ice cover appeared to be enriched in GHGs compared to the water column. This enrichment is due to the concentration effect, associated with sea ice growth, of already enriched parent seawater and/or enriched riverine freshwater. As sea ice temperature and brine volume decreases, the solubility of GHGs trapped within the ice matrix decreases, leading to bubble formation. In addition, gas bubbles originating from the sediment may be incorporated within the ice cover and contribute to the sea ice enrichment in GHGs. Due to the low brine volume of brackish sea ice, bubbles accumulated in the ice matrix are expected to remain until the onset of sea ice melt. This temporary GHG storage in sea ice may have implications for the magnitude and timing of the BB GHG fluxes, which would be further constrained if sea ice supports active microbial CH_4 oxidation.

Data accessibility statement

Data are available at HydroShare: https://doi.org/10.4211/hs.13f2735419cf4d2cac8ab353725e3145.

Acknowledgments

This research was primarily funded by the International Union for Conservation of Nature, with additional financial support from the Canadian Natural Sciences and Engineering Research Council and the Canada Foundation for Innovation. BD is a research associate of the F.R.S-FNR. The authors would like to thank Jody Deming, Mats Granskog, and an anonymous reviewer for their constructive comments that greatly improved the overall quality of the article.

Funding

Financial support for this study was provided by the Canada Excellence Research Chairs program, the Canada Research Chairs program, the Natural Sciences and Engineering Research Council, and the Canada Foundation for Innovation. E-ER is funded by the Academy of Finland (PRICE 325140). The study utilized SYKE marine research infrastructure as a part of the national FINMARI RI consortium.

Competing interests

The authors declare no competing interests.

Author contributions

Field sampling was performed by N-XG, KMM, HK, E-ER. Laboratory and data analyses were performed by N-XG, ML, BD. All authors contributed to the article redaction and have reviewed and approved the submitted version for publication.

References

Anderson, IC, Levine, JS. 1986. Relative rates of nitric oxide and nitrous oxide production by nitrifiers, denitrifiers, and nitrate respirers. *Applied Environmental Microbiology* **51**(5): 938–945. DOI: http://dx.doi.org/10.1128/AEM.51.5.938-945.1986.

Arctic Monitoring and Assessment Programme. 2015. AMAP assessment 2015: Methane as an Arctic climate forcer. Oslo, Norway: Arctic Monitoring and Assessment Programme (AMAP), pp. vii + 139.

Arrigo, KR. 2017. Sea ice as a habitat for primary producers, in Thomas, DN ed., *Sea ice*. UK: John Wiley: 352–369. DOI: http://dx.doi.org/10.1002/9781118778371.ch14.

Bakker, DCE, Bange, HW, Gruber, N, Johannessen, T, Upstill-Goddard, RC, Borges, AV, Delille, B, Löscher, CR, Naqvi, SWA, Omar, AM, Santana-Casiano, JM. 2014. Air-sea interactions of natural long-lived greenhouse gases (CO_2, N_2O, CH_4) in a changing climate, in Liss, PS, Johnson, MT eds., *Ocean-atmosphere interactions of gases and particles*. Berlin, Heidelberg: Springer: 113–169. DOI: http://dx.doi.org/10.1007/978-3-642-25643-1_3.

Bange, HW, Bartell, UH, Rapsomanikis, S, Andreae, MO. 1994. Methane in the Baltic and North Seas and a reassessment of the marine emissions of methane. *Global Biogeochemical Cycles* **8**(4): 465–480. DOI: http://dx.doi.org/10.1029/94GB02181.

Beldowski, J, Löffler, A, Schneider, B, Joensuu, L. 2010. Distribution and biogeochemical control of total CO_2 and total alkalinity in the Baltic Sea. *Journal of Marine Systems* **81**(3): 252–259. DOI: http://dx.doi.org/10.1016/j.jmarsys.2009.12.020.

Bluhm, BA, Swadling, KM, Gradinger, R. 2017. Sea ice as a habitat for macrograzers, in Thomas, DN ed., *Sea ice*. UK: John Wiley: 394–414. DOI: http://dx.doi.org/10.1002/9781118778371.ch16.

Borges, AV. 2005. Do we have enough pieces of the jigsaw to integrate CO_2 fluxes in the coastal ocean? *Estuaries* **28**(1): 3–27. DOI: http://dx.doi.org/10.1007/BF02732750.

Borges, AV, Champenois, W, Gypens, N, Delille, B, Harlay, J. 2016. Massive marine methane emissions from near-shore shallow coastal areas. *Scientific Reports* **6**(1): 1–8. DOI: http://dx.doi.org/10.1038/srep27908.

Bowman, JS, Rasmussen, S, Blom, N, Deming, JW, Rysgaard, S, Sicheritz-Ponten, T. 2012. Microbial community structure of Arctic multiyear sea ice and surface seawater by 454 sequencing of the 16S RNA gene. *ISME Journal* **6**(1): 11–20. DOI: http://dx.doi.org/10.1038/ismej.2011.76.

Carini, P, White, AE, Campbell, EO, Giovannoni, SJ. 2014. Methane production by phosphate-starved SAR11 chemoheterotrophic marine bacteria. *Nature Communications* **5**(1): 4346. DOI: http://dx.doi.org/10.1038/ncomms5346.

Caron, DA, Gast, RJ, Garneau, M-È. 2017. Sea ice as a habitat for micrograzers, in Thomas, DN ed., *Sea*

ice. UK: John Wiley. DOI: http://dx.doi.org/10.1002/9781118778371.ch15.

Cox, GFN, Weeks, WF. 1983. Equations for determining the gas and brine volumes in sea-ice samples. *Journal of Glaciology* **29**(102): 306–316. DOI: http://dx.doi.org/10.3189/S0022143000008364.

Crabeck, O, Delille, B, Thomas, D, Geilfus, NX, Rysgaard, S, Tison, JL. 2014. CO_2 and CH_4 in sea ice from a Subarctic fjord under influence of riverine input. *Biogeosciences* **11**(23): 6525–6538. DOI: http://dx.doi.org/10.5194/bg-11-6525-2014.

Crabeck, O, Galley, RJ, Mercury, L, Delille, B, Tison, JL, Rysgaard, S. 2019. Evidence of freezing pressure in sea ice discrete brine inclusions and its impact on aqueous-gaseous equilibrium. *Journal of Geophysical Research: Oceans* **124**(3): 1660–1678. DOI: http://dx.doi.org/10.1029/2018JC014597.

Damm, E, Rudels, B, Schauer, U, Mau, S, Dieckmann, G. 2015. Methane excess in Arctic surface water-triggered by sea ice formation and melting. *Scientific Reports* **5**: 16179. DOI: http://dx.doi.org/10.1038/srep16179.

Deming, JW, Collins, E. 2017. Sea ice as a habitat for Bacteria, Archaea and viruses, in Thomas, DN ed., *Sea ice*. UK: John Wiley: 326–351. DOI: http://dx.doi.org/10.1002/9781118778371.ch13.

Dieckmann, GS, Nehrke, G, Papadimitriou, S, Gottlicher, J, Steininger, R, Kennedy, H, Wolf-Gladrow, D, Thomas, DN. 2008. Calcium carbonate as ikaite crystals in Antarctic sea ice. *Geophysical Research Letters* **35**(8): L08501. DOI: http://dx.doi.org/10.1029/2008GL033540.

Eicken, H. 2003. From the microscopic, to the macroscopic, to the regional scale: Growth, microstructure and properties of sea ice, in Thomas, DN ed., *Sea ice*. UK: John Wiley: 22–81. DOI: http://dx.doi.org/10.1002/9780470757161.ch2.

Frankignoulle, M, Abril, G, Borges, A, Bourge, I, Canon, C, Delille, B, Libert, E, Théate, JM. 1998. Carbon dioxide emission from European Estuaries. *Science* **282**(5388): 434–436. DOI: http://dx.doi.org/10.1126/science.282.5388.434.

Fransson, A, Chierici, M, Abrahamsson, K, Andersson, M, Granfors, A, Gårdfeldt, K, Torstensson, A, Wulff, A. 2015. CO_2-system development in young sea ice and CO_2 gas exchange at the ice/air interface mediated by brine and frost flowers in Kongsfjorden, Spitsbergen. *Annals of Glaciology* **56**(69): 245–257. DOI: http://dx.doi.org/10.3189/2015AoG69A563.

Fransson, A, Chierici, M, Skjelvan, I, Olsen, A, Assmy, P, Peterson, AK, Spreen, G, Ward, B. 2017. Effects of sea-ice and biogeochemical processes and storms on under-ice water fCO_2 during the winter-spring transition in the high Arctic Ocean: Implications for sea-air CO_2 fluxes. *Journal of Geophysical Research: Oceans* **122**(7): 5566–5587. DOI: http://dx.doi.org/10.1002/2016JC012478.

Geilfus, NX, Carnat, G, Dieckmann, GS, Halden, N, Nehrke, G, Papakyriakou, TN, Tison, JL, Delille, B. 2013. First estimates of the contribution of $CaCO_3$ precipitation to the release of CO_2 to the atmosphere during young sea ice growth. *Journal of Geophysical Research: Oceans* **118**: 244–255. DOI: http://dx.doi.org/10.1029/2012JC007980.

Geilfus, NX, Carnat, G, Papakyriakou, T, Tison, JL, Else, B, Thomas, H, Shadwick, E, Delille, B. 2012. Dynamics of pCO_2 and related air-ice CO_2 fluxes in the Arctic coastal zone (Amundsen Gulf, Beaufort Sea). *Journal of Geophysical Research: Oceans* **117**(C9). DOI: http://dx.doi.org/10.1029/2011JC007118.

Geilfus, NX, Galley, RJ, Crabeck, O, Papakyriakou, T, Landy, J, Tison, JL, Rysgaard, S. 2015. Inorganic carbon dynamics of melt-pond-covered first-year sea ice in the Canadian Arctic. *Biogeosciences* **12**(6): 2047–2061. DOI: http://dx.doi.org/10.5194/bg-12-2047-2015.

Geilfus, NX, Galley, RJ, Else, BGT, Campbell, K, Papakyriakou, T, Crabeck, O, Lemes, M, Delille, B, Rysgaard, S. 2016. Estimates of ikaite export from sea ice to the underlying seawater in a sea ice–seawater mesocosm. *The Cryosphere* **10**(5): 2173–2189. DOI: http://dx.doi.org/10.5194/tc-10-2173-2016.

Geilfus, NX, Munson, KM, Lemes, M, Wang, F, Tison, JL, Rysgaard, S. 2021. Meteoric water contribution to sea ice formation and its control of the surface water carbonate cycle in the Wandel Sea shelf, northeastern Greenland. *Elementa: Science of the Anthropocene* **9**(1). DOI: http://dx.doi.org/10.1525/elementa.2021.00004.

Geilfus, NX, Munson, KM, Sousa, J, Germanov, Y, Bhugaloo, S, Babb, D, Wang, F. 2019. Distribution and impacts of microplastic incorporation within sea ice. *Marine Pollution Bulletin* **145**: 463–473. DOI: http://dx.doi.org/10.1016/j.marpolbul.2019.06.029.

Golden, KM, Eicken, H, Heaton, AL, Miner, J, Pringle, DJ, Zhu, J. 2007. Thermal evolution of permeability and microstructure in sea ice. *Geophysical Research Letters* **34**(L16501). DOI: http://dx.doi.org/10.1029/2007GL030447.

Gran, G. 1952. Determination of the equivalence point in potentiometric titration. Part II. *Analyst* **77**: 661–671. DOI: http://dx.doi.org/10.1039/an9527700661.

Granskog, MA, Kaartokallio, H, Kuosa, H, Thomas, DN, Vainio, J. 2006a. Sea ice in the Baltic Sea—A review. *Estuarine, Coastal Shelf Science* **70**(1): 145–160. DOI: http://dx.doi.org/10.1016/j.ecss.2006.06.001.

Granskog, MA, Martma, TA, Vaikmäe, RA. 2003. Development, structure and composition of land-fast sea ice in the northern Baltic Sea. *Journal of Glaciology* **49**(164): 139–148. DOI: http://dx.doi.org/10.3189/172756503781830872.

Granskog, MA, Uusikivi, J, Blanco Sequeiros, A, Sonninen, E. 2006b. Relation of ice growth rate to salt segregation during freezing of low-salinity sea water (Bothnian Bay, Baltic Sea). *Annals of Glaciology*

44(1), 134–138. DOI: http://dx.doi.org/10.3189/172756406781811259.

Granskog, MA, Virkkunen, K, Thomas, DN, Ehn, J, Kola, H, Martma, T. 2004. Chemical properties of brackish water ice in the Bothnian Bay, the Baltic Sea. *Journal of Glaciology* **50**(169): 292–302. DOI: http://dx.doi.org/10.3189/172756504781830079.

Grasshoff, K, Ehrhardt, M, Kremling, K eds. 1983. *Methods of seawater analysis*. Weinheim, Germany: Verlag Chemie.

Heeschen, KU, Collier, RW, de Angelis, MA, Suess, E, Rehder, G, Linke, P, Klinkhammer, GP. 2005. Methane sources, distributions, and fluxes from cold vent sites at Hydrate Ridge, Cascadia margin. *Global Biogeochemical Cycles* **19**(2). DOI: http://dx.doi.org/10.1029/2004gb002266.

Hjalmarsson, S, Wesslander, K, Anderson, LG, Omstedt, A, Perttilä, M, Mintrop, L. 2008. Distribution, long-term development and mass balance calculation of total alkalinity in the Baltic Sea. *Continental Shelf Research* **28**(4): 593–601. DOI: http://dx.doi.org/10.1016/j.csr.2007.11.010.

Hu, YB, Wang, F, Boone, W, Barber, D, Rysgaard, S. 2018. Assessment and improvement of the sea ice processing for dissolved inorganic carbon analysis. *Limnology and Oceanography: Methods* **16**(2): 83–91. DOI: http://dx.doi.org/10.1002/lom3.10229.

Humborg, C, Geibel, MC, Sun, X, McCrackin, M, Mörth, CM, Stranne, C, Jakobsson, M, Gustafsson, B, Sokolov, A, Norkko, A, Norkko, J. 2019. High emissions of carbon dioxide and methane from the coastal Baltic Sea at the end of a summer heat wave. *Frontiers in Marine Science* **6**. DOI: http://dx.doi.org/10.3389/fmars.2019.00493.

Kaartokallio, H. 2001. Evidence for active microbial nitrogen transformations in sea ice (Gulf of Bothnia, Baltic Sea) in midwinter. *Polar Biology* **24**(1): 21–28. DOI: http://dx.doi.org/10.1007/s003000000169.

Kaartokallio, H. 2004. Food web components, and physical and chemical properties of Baltic Sea ice. *Marine Ecology Progress Series* **273**: 49–63. DOI: http://dx.doi.org/10.3354/meps273049.

Karl, DM, Beversdorf, L, Björkman, KM, Church, MJ, Martinez, A, Delong, EF. 2008. Aerobic production of methane in the sea. *Nature Geosciences* **1**(7): 473–478. DOI: http://dx.doi.org/10.1038/ngeo234.

Kawamura, T, Shirasawa, K, Ishikawa, N, Lindfors, A, Rasmus, K, Granskog, MA, Ehn, J, Leppäranta, M, Martha, T, Vaikmäe, R. 2001. Time-series observations of the structure and properties of brackish ice in the Gulf of Finland. *Annals of Glaciology* **33**: 1–4. DOI: http://dx.doi.org/10.3189/172756401781818950.

Kitidis, V, Upstill-Goddard, RC, Anderson, LG. 2010. Methane and nitrous oxide in surface water along the North-West Passage, Arctic Ocean. *Marine Chemistry* **121**(1): 80–86. DOI: http://dx.doi.org/10.1016/j.marchem.2010.03.006.

Knittel, K, Boetius, A. 2009. Anaerobic oxidation of methane: Progress with an unknown process. *Annual Review of Microbiology* **63**: 311–334. DOI: http://dx.doi.org/10.1146/annurev.micro.61.080706.093130.

Kuosa, H, Kaartokallio, H. 2006. Experimental evidence on nutrient and substrate limitation of Baltic Sea sea-ice algae and bacteria. *Hydrobiologia* **554**(1): 1–10. DOI: http://dx.doi.org/10.1007/s10750-005-1001-z.

Kvenvolden, KA, Lilley, MD, Lorenson, TD, Barnes, PW, McLaughlin, E. 1993. The Beaufort Sea continental shelf as a seasonal source of atmospheric methane. *Geophysical Research Letters* **20**(22): 2459–2462. DOI: http://dx.doi.org/10.1029/93gl02727.

Lannuzel, D, Tedesco, L, van Leeuwe, M, Campbell, K, Flores, H, Delille, B, Miller, L, Stefels, J, Assmy, P, Bowman, J, Brown, K, Castellani, G, Chierici, M, Crabeck, O, Damm, E, Else, B, Fransson, A, Fripiat, F, Geilfus, NX, Jacques C, Jones, E, Kaartokallio, H, Kotovitch, M, Meiners, K, Moreau, S, Nomura, D, Peeken, I, Rintala, JM, Steiner, N, Tison, JL, Vancoppenolle, M, Van der Linden, F, Vichi, M, Wongpan, P. 2020. The future of Arctic sea-ice biogeochemistry and ice-associated ecosystems. *Nature Climate Change* **10**(11): 983–992. DOI: http://dx.doi.org/10.1038/s41558-020-00940-4.

Leppäranta, M, Manninen, T. 1988. The brine and gas content of sea ice with attention to low salinities and high temperatures. *Finnish Institute Marine Research Internal Report* **88**: 2.

Löffler, A, Schneider, B, Perttilä, M, Rehder, G. 2012. Air–sea CO_2 exchange in the Gulf of Bothnia, Baltic Sea. *Continental Shelf Research* **37**: 46–56. DOI: http://dx.doi.org/10.1016/j.csr.2012.02.002.

Myllykangas, JP, Hietanen, S, Jilbert, T. 2021. Legacy effects of eutrophication on modern methane dynamics in a boreal estuary. *Estuaries and Coasts* **43**(2): 189–206. DOI: http://dx.doi.org/.1007/s12237-019-00677-0.

Op den Camp, HJM, Islam, T, Stott, MB, Harhangi, HR, Hynes, A, Schouten, S, Jetten, MSM, Birkeland, NK, Pol, A, Dunfield, PF. 2009. Environmental, genomic and taxonomic perspectives on methanotrophic Verrucomicrobia. *Environmental Microbiology Reports* **1**(5): 293–306. DOI: http://dx.doi.org/10.1111/j.1758-2229.2009.00022.x.

Papadimitriou, S, Kennedy, H, Kennedy, DP, Thomas, DN. 2013. Ikaite solubility in seawater-derived brines at 1 atm and sub-zero temperatures to 265 K. *Geochemica et Cosmochimica Acta* **109**(15). DOI: http://dx.doi.org/10.1016/j.gca.2013.01.044.

Parmentier, FJW, Christensen, TR, Rysgaard, S, Bendtsen, J, Glud, RN, Else, B, van Huissteden, J, Sachs, T, Vonk, JE, Sejr, MK. 2017. A synthesis of the arctic terrestrial and marine carbon cycles under pressure from a dwindling cryosphere. *Ambio* **46**(1): 53–69. DOI: http://dx.doi.org/10.1007/s13280-016-0872-8.

Pomeroy, L, Wiebe, W. 2001. Temperature and substrates as interactive limiting factors for marine heterotrophic bacteria. *Aquatic Microbial Ecology* **23**(2): 187–204. DOI: http://dx.doi.org/10.3354/ame023187.

Puri, AW, Owen, S, Chu, F, Chavkin, T, Beck, DAC, Kalyuzhnaya, MG, Lidstrom, ME. 2015. Genetic tools for the industrially promising methanotroph *Methylomicrobium buryatense*. *Applied and Environmental Microbiology* **81**(5): 1775–1781. DOI: http://dx.doi.org/10.1128/AEM.03795-14.

Randall, K, Scarratt, M, Levasseur, M, Michaud, S, Xie, H, Gosselin, M. 2012. First measurements of nitrous oxide in Arctic sea ice. *Journal of Geophysical Research: Oceans* **117**(C00G15). DOI: http://dx.doi.org/doi:10.1029/2011JC007340.

Reeburgh, WS. 2007. Oceanic methane biogeochemistry. *Chemical Reviews* **107**(2): 486–513. DOI: http://dx.doi.org/10.1021/cr050362v.

Riedel, A, Michel, C, Gosselin, M. 2007. Grazing of large-sized bacteria by sea-ice heterotrophic protists on the Mackenzie Shelf during the winter-spring transition. *Aquatic Microbial Ecology* **50**(1): 25–38. DOI: http://dx.doi.org/10.3354/ame01155.

Rysgaard, S, Bendtsen, J, Delille, B, Dieckmann, GS, Glud, RN, Kennedy, H, Mortensen, J, Papadimitriou, S, Thomas, DN, Tison, JL. 2011. Sea ice contribution to the air-sea CO_2 exchange in the Arctic and Southern Oceans. *Tellus Series B: Chemical and Physical Meteorology* **63**(5): 823–830. DOI: http://dx.doi.org/10.1111/j.1600-0889.2011.00571.x.

Rysgaard, S, Bendtsen, J, Pedersen, LT, Ramlov, H, Glud, RN. 2009. Increased CO_2 uptake due to sea ice growth and decay in the Nordic Seas. *Journal of Geophysical Research: Oceans* **114**(C09011). DOI: http://dx.doi.org/10.1029/2008JC005088.

Rysgaard, S, Glud, RN, Sejr, MK, Bendtsen, J, Christensen, PB. 2007. Inorganic carbon transport during sea ice growth and decay: A carbon pump in polar seas. *Journal of Geophysical Research: Oceans* **112**: C03016. DOI: http://dx.doi.org/10.1029/2006JC003572.

Rysgaard, S, Søgaard, DH, Cooper, M, Pućko, M, Lennert, K, Papakyriakou, TN, Wang, F, Geilfus, NX, Glud, RN, Ehn, J, McGinnis, DF, Attard, K, Sievers, J, Deming, JW, Barber, D. 2013. Ikaite crystal distribution in winter sea ice and implications for CO_2 system dynamics. *The Cryosphere* **7**(2): 707–718. DOI: http://dx.doi.org/10.5194/tc-7-707-2013.

Schmale, O, Schneider von Deimling, J, Gülzow, W, Nausch, G, Waniek, JJ, Rehder, G. 2010. Distribution of methane in the water column of the Baltic Sea. *Geophysical Research Letters* **37**(12). DOI: http://dx.doi.org/10.1029/2010GL043115.

Schneider, B. 2011. The CO_2 system of the Baltic Sea: Biogeochemical control and impact of anthropogenic CO_2, in Schernewski, G, Hofstede, J, Neumann, T ed., *Global change and Baltic coastal zones*. The Netherlands: Springer: 33–49. DOI: http://dx.doi.org/10.1007/978-94-007-0400-8_3.

Shakhova, N, Semiletov, I, Leifer, I, Salyuk, A, Rekant, P, Kosmach, D. 2010. Geochemical and geophysical evidence of methane release over the East Siberian Arctic Shelf. *Journal of Geophysical Research: Oceans* **115**(C8). DOI: http://dx.doi.org/10.1029/2009JC005602.

Silvennoinen, H, Liikanen, A, Rintala, J, Martikainen, PJ. 2008. Greenhouse gas fluxes from the eutrophic Temmesjoki river and its estuary in the Liminganlahti Bay (the Baltic Sea). *Biogeochemistry* **90**(2): 193–208. DOI: http://dx.doi.org/10.1007/s10533-008-9244-1.

Tison, JL, Schwegmann, S, Dieckmann, G, Rintala, JM, Meyer, H, Moreau, S, Vancoppenolle, M, Nomura, D, Engberg, S, Blomster, LJ, Hendricks, S, Uhlig, C, Luhtanen, AM, de jong, J, Janssens, J, Carnat, G, Zhou, J, Delille, B. 2017. Biogeochemical impact of snow cover and cyclonic intrusions on the winter Weddell Sea ice pack. *Journal of Geophysical Research: Oceans* **122**(12): 9548–9571. DOI: http://dx.doi.org/10.1002/2017JC013288.

Tušer, M, Picek, T, Sajdlová, Z, Jůza, T, Muška, M, Frouzová, J. 2017. Seasonal and spatial dynamics of gas ebullition in a temperate water-storage reservoir. *Water Resources Research* **53**(10): 8266–8276. DOI: http://dx.doi.org/10.1002/2017WR020694.

Tyrrell, T, Schneider, B, Charalampopoulou, A, Riebesell, U. 2008. Coccolithophores and calcite saturation state in the Baltic and Black Seas. *Biogeosciences* **5**(2): 485–494. DOI: http://dx.doi.org/10.5194/bg-5-485-2008.

Van der Linden, FC, Tison, JL, Champenois, W, Moreau, S, Carnat, G, Kotovitch, M, Fripiat, F, Deman, F, Roukaerts, A, Dehairs, F, Wauthy, S, Lourenço, A, Vivier, F, Haskell, T, Delille, B. 2020. Sea ice CO_2 dynamics across seasons: Impact of processes at the interfaces. *Journal of Geophysical Research: Oceans* **125**(6). DOI: http://dx.doi.org/10.1029/2019JC015807.

Verdugo, J, Damm, E, Snoeijs, P, Díez, B, Farías, L. 2016. Climate relevant trace gases (N_2O and CH_4) in the Eurasian Basin (Arctic Ocean). *Deep Sea Research Part I: Oceanographic Research Papers* **117**, 84–94. DOI: http://dx.doi.org/10.1016/j.dsr.2016.08.016.

Vihma, T, Haapala, J. 2015. Geophysics of sea ice in the Baltic Sea: A review. *Progress in Oceanography* **80**(3–4), 129–148. DOI: http://dx.doi.org/10.1016/j.pocean.2009.02.002.

Weiss, RF, Price, BA. 1980. Nitrous oxide solubility in water and seawater. *Marine Chemistry* **8**: 347–359. DOI: http://dx.doi.org/10.1016/0304-4203(80)90024-9.

Wiesenburg, DA, Guinasso, NL. 1979. Equilibrium solubilities of methane, carbon monoxide, and hydrogen in water and sea water. *Journal of Chemical and Engineering Data* **24**(4): 356–360. DOI: http://dx.doi.org/10.1021/je60083a006.

Wilkinson, J, Maeck, A, Alshboul, Z, Lorke, A. 2015. Continuous seasonal river ebullition measurements linked to sediment methane formation. *Environmental Science and Technology* **49**(22):

13121–13129. DOI: http://dx.doi.org/10.1021/acs.est.5b01525.

Zhou, JY, Delille, B, Eicken, H, Vancoppenolle, M, Brabant, F, Carnat, G, Geilfus, NX, Papakyriakou, T, Heinesch, B, Tison, JL. 2013. Physical and biogeochemical properties in landfast sea ice (Barrow, Alaska): Insights on brine and gas dynamics across seasons. *Journal of Geophysical Research: Oceans* **118**(6): 3172–3189. DOI: http://dx.doi.org/10.1002/jgrc.20232.

Zhou, JY, Tison, JL, Carnat, G, Geilfus, NX, Delille, B. 2014. Physical controls on the storage of methane in landfast sea ice. *The Cryosphere* **8**(3): 1019–1029. DOI: http://dx.doi.org/10.5194/tc-8-1019-2014.

How to cite this article: Geilfus, N-X, Munson, KM, Eronen-Rasimus, E, Kaartokallio, H, Lemes, M, Wang, F, Rysgaard, S, Delille, B. 2021. Landfast sea ice in the Bothnian Bay (Baltic Sea) as a temporary storage compartment for greenhouse gases. *Elementa: Science of the Anthropocene* 9(1). DOI: https://doi.org/10.1525/elementa.2021.00028

Domain Editor-in-Chief: Jody W. Deming, University of Washington, Seattle, WA, USA

Associate Editor: Stephen F. Ackley, Department of Geological Sciences, University of Texas at San Antonio, TX, USA

Knowledge Domain: Ocean Science

Part of an Elementa Special Feature: Insights into Biogeochemical Exchange Processes at Sea Ice Interfaces (BEPSII-2)

Published: November 18, 2021 **Accepted:** October 19, 2021 **Submitted:** April 12, 2021

ELEMENTA Science of the Anthropocene

Elem Sci Anth is a peer-reviewed open access journal published by University of California Press.

OPEN ACCESS